

5-Methyltetrahydrofolate Is Bound in Intersubunit Areas of Rat Liver Folate-binding Protein Glycine *N*-Methyltransferase*

Received for publication, November 7, 2006, and in revised form, December 5, 2006. Published, JBC Papers in Press, December 7, 2006, DOI 10.1074/jbc.M610384200

Zigmund Luka[‡], Svetlana Pakhomova[§], Lioudmila V. Loukachevitch[‡], Martin Egli[‡], Marcia E. Newcomer[§], and Conrad Wagner^{‡¶1}

From the [‡]Department of Biochemistry, Vanderbilt University School of Medicine, Nashville, Tennessee 37232, [¶]Veterans Affairs Medical Center, Nashville, Tennessee 37212, and [§]Department of Biological Sciences, Louisiana State University, Baton Rouge, Louisiana 70803

Glycine *N*-methyltransferase (GNMT) is a key regulatory enzyme in methyl group metabolism. It is abundant in the liver, where it uses excess *S*-adenosylmethionine (AdoMet) to methylate glycine to *N*-methylglycine (sarcosine) and produces *S*-adenosylhomocysteine (AdoHcy), thereby controlling the methylating potential of the cell. GNMT also links utilization of preformed methyl groups, in the form of methionine, to their *de novo* synthesis, because it is inhibited by a specific form of folate, 5-methyltetrahydrofolate. Although the structure of the enzyme has been elucidated by x-ray crystallography of the apoenzyme and in the presence of the substrate, the location of the folate inhibitor in the tetrameric structure has not been identified. We report here for the first time the crystal structure of rat GNMT complexed with 5-methyltetrahydrofolate. In the GNMT-folate complex, two folate binding sites were located in the intersubunit areas of the tetramer. Each folate binding site is formed primarily by two 1–7 N-terminal regions of one pair of subunits and two 205–218 regions of the other pair of subunits. Both the pteridine and *p*-aminobenzoyl rings are located in the hydrophobic cavities formed by Tyr⁵, Leu²⁰⁷, and Met²¹⁵ residues of all subunits. Binding experiments in solution also confirm that one GNMT tetramer binds two folate molecules. For the enzymatic reaction to take place, the N-terminal fragments of GNMT must have a significant degree of conformational freedom to provide access to the active sites. The presence of the folate in this position provides a mechanism for its inhibition.

The methylation of nucleic acids, proteins, and small molecules in the cells is one of the most important ways of modulating metabolism and development. Each methylation reaction is carried out by a specific enzyme, but all such reactions are

dependent on the concentrations of the substrate, AdoMet,² and of the product of the reaction, AdoHcy. That ratio AdoMet/AdoHcy is considered an index of the methylation capacity of the cell (1, 2).

One of the key regulatory elements in maintaining the AdoMet/AdoHcy ratio is the enzyme glycine *N*-methyltransferase (3, 4). This enzyme, which catalyzes the methylation of glycine, is considered to be a tool for the removal of an excess of AdoMet when its concentration in the cell is increased (increased dietary methionine). Inactivation of GNMT by missense mutations in human individuals resulted in highly elevated concentrations of AdoMet and methionine in the patient's plasma (5, 6). Model mice with the *Gnmt* gene completely knocked out have an extremely high concentration of AdoMet and a high ratio of AdoMet/AdoHcy in the liver (7).

An important finding was made when a major folate-binding protein in rat liver cytosol was identified as GNMT (8–10). That discovery immediately raised questions as to how this enzyme operates in the cell in the presence of folate, how GNMT is related to folate metabolism, and what is the biological role of the enzyme. A unique property of GNMT methyltransferase is that it was found that binding of the 5-methyltetrahydrofolate pentaglutamate (5-CH₃-H₄PteGlu₅) inhibits methyltransferase activity of GNMT (11). This confers a special role for the enzyme by which it links the activity of the enzyme in the transfer of preformed methyl groups arising from methionine via AdoMet to the *de novo* synthesis of methyl groups by way of the folate one-carbon pool. A regulatory scheme was proposed in which GNMT not only maintains the AdoMet/AdoHcy ratio but also controls methyl group synthesis (12). The structure of the GNMT-folate complex is obviously of great importance, but until now, no such crystal structure was available.

The crystal structures of the rat, mouse, and human GNMT apoproteins (13, 14) are known as well as the rat GNMT complexed either with AdoMet or complexed with AdoHcy (15–17). The overall structures of GNMTs from various species are very similar. All enzymes are tetramers of flat shape with numerous contacts between subunits and lower density in the center of the tetramer (see Fig. 1). Each

* This work was supported by National Institutes of Health Grants DK15289 (to C. W.) and GM55237 (to M. E.) and from Louisiana Governor's Biotechnology Initiative (to M. E. N.). The costs of publication of this article were defrayed in part by the payment of page charges. This article must therefore be hereby marked "advertisement" in accordance with 18 U.S.C. Section 1734 solely to indicate this fact.

The atomic coordinates and structure factors (code 2IDJ and 2IDK) have been deposited in the Protein Data Bank, Research Collaboratory for Structural Bioinformatics, Rutgers University, New Brunswick, NJ (<http://www.rcsb.org/>).

¹ To whom correspondence should be addressed: Dept. of Biochemistry, Vanderbilt University Medical Ctr., 620 Light Hall, Nashville, TN 37232. Tel.: 615-343-9866; Fax: 615-343-0407; E-mail: Conrad.Wagner@vanderbilt.edu.

² The abbreviations and trivial names used are: AdoMet, *S*-adenosylmethionine; GNMT, glycine *N*-methyltransferase; AdoHcy, *S*-adenosylhomocysteine; 5-CH₃-H₄PteGlu, 5-methyltetrahydrofolate monoglutamate; TCEP, tris(2-carboxyethyl)phosphine hydrochloride; PABA, *p*-aminobenzoic acid.

GNMT-Folate Structure

subunit possesses an active center where AdoMet and glycine are bound deep inside of the globular part of the subunits. The enzymatic reaction starts with the AdoMet binding, which leads to significant conformational changes, especially in the N-terminal parts of each monomer, as shown by crystallization of rat GNMT with AdoMet, AdoMet with acetate anion, and by the kinetic data (16–17). The active centers of GNMT could bind some other compounds as shown in the crystal structures of the human and mouse enzymes, where Tris or citrate molecules from the mother liquors were found (14). By protein-ligand docking modeling, it was shown that benzopyrene could potentially bind to the active center of GNMT (18). Does that mean that folates could also bind to the active center, as proposed earlier (15)?

The crystal structure determination of the folate-GNMT complex now provides insight to the mechanism and specificity of inhibition by folate and its link to one-carbon metabolism in the cell. In this work, we report the crystal structure of rat GNMT complexed with 5-methyltetrahydrofolate.

EXPERIMENTAL PROCEDURES

GNMT Preparation—All experiments in this work were done with rat GNMT, as this enzyme was discovered as the folate-binding protein in rat liver, and folate binding *in vitro* has been described for this enzyme (11). In addition, the crystal structure of the rat enzyme has been relatively well studied (13, 15–17). Rat GNMT was expressed in *E. coli* and purified as reported earlier (19). Briefly, rat GNMT cDNA was cloned in pET-17b expression vector and expressed in the BL21(GE3) *E. coli* strain. After preparation of the crude extract, GNMT was purified by ammonium sulfate precipitation, DE-52 anion exchange chromatography, and Sephacryl S-200 size exclusion chromatography. Protein of 96–98% purity was used for crystallization and other experiments.

Folate Binding—All experiments of folate binding and crystallization were done with (6S)-5-methyltetrahydrofolate monoglutamate ((6S)-5-CH₃-H₄PteGlu, hereafter referred to as folate) (Fig. 1) from Merck EPROVA AG, Schaffhausen, Switzerland. This derivative of folic acid was used because it is a basic natural form of folate, it is available in large quantities suitable for crystallization studies, and it has been shown to inhibit and bind to the rat liver enzyme (11, 20). Binding to GNMT was measured by a filtration method. The rat enzyme was incubated with folate in 20 mM Tris, 25 mM NaCl, and 5 mM Tris(2-carboxyethyl)phosphine hydrochloride (TCEP), pH 7.5, for 1 h. The material was placed into a Microcon YM-10 concentrator (Amicon Bio-separation), and a small volume of the solvent with unbound folate was quickly separated by centrifugation. Concentration of folate in the filtrate [F_{free}] was measured by absorbance at 290 nm (maximum for folate at neutral pH) by using a molar extinction coefficient of 3.17×10^4 (21). Subtracting the free concentration of folate from the total concentration gave us the concentration of bound folate [F_{bound}]. The molar ratio of [F_{bound}]/[GNMT_{tetr}] (*V*), with [GNMT_{tetr}] as a molar concentration of GNMT tetramer, was plotted against [F_{free}], and the resulting plot was fitted with the following

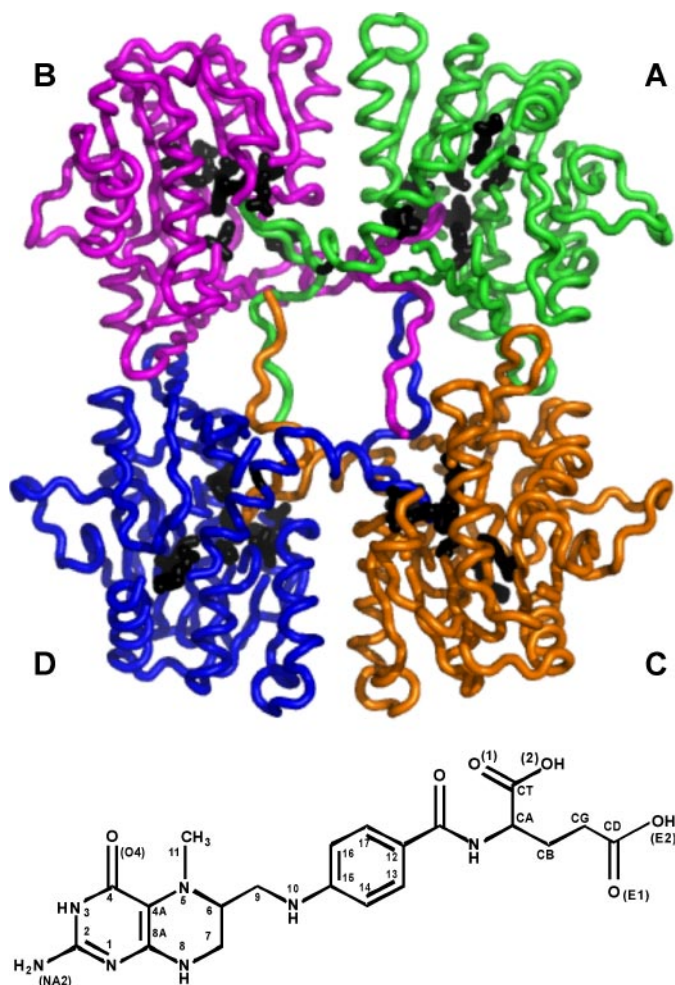


FIGURE 1. Structures of GNMT and (6S)-5-CH₃-H₄PteGlu. The GNMT apoprotein structure is that obtained in this work (PDB accession code 2IDJ). Protein subunits A, B, C, and D are shown in green, magenta, orange, and blue, respectively. The side chains of residues in active centers participating in the interactions with AdoMet (PDB accession code 1NBH; Ref. 17) are shown in black.

equation: $V = nK_A[F_{\text{free}}]/(1 - K_A[F_{\text{free}}])$ (by KaleidaGraph (Synergy Software) non-linear fitting algorithm according to Refs. 22 and 23). The *n* and *K_A* parameters are the total number of ligand molecules bound to GNMT tetramer and an association constant, respectively.

Crystallization—The GNMT-folate complex was crystallized by the sitting drop method at room temperature. The protein (4–6 mg/ml concentration in 20 mM Tris-HCl, pH 7.5, 25 mM NaCl, 5 mM TCEP) was incubated with 1–3 mM folate for at least 1 h prior to the crystallization. The protein-folate complex was mixed with the reservoir solution (20% polyethylene glycol 3350, 0.2 M calcium-acetate). The crystals of the GNMT-folate complex appeared in a few hours and grew to the maximum dimensions in 4–6 days. They belong to the monoclinic P₂₁ space group with *a* = 57.869, *b* = 85.223, and *c* = 131.861 Å and $\beta = 91.40^\circ$. Crystals of the GNMT apoprotein were grown from the same conditions, with folate being omitted from the crystallization, and they are isomorphous with the GNMT-folate crystals.

X-ray Data Collection—Prior to the data collection, a suitable crystal was dipped for several seconds in a modified mother

TABLE 1
Data collection and refinement statistics

	GNMT apoprotein	GNMT-folate complex
Data collection		
Resolution (Å)	50-2.35	50-2.55
Space group	P ₂ ₁	P ₂ ₁
Cell dimensions		
<i>a</i> (Å)	57.869	57.427
<i>b</i> (Å)	85.223	84.751
<i>c</i> (Å)	131.861	132.245
β (°)	91.40	91.61
Unique reflections	53 782	38 846
<i>R</i> _{sym} ^{a,b} (%)	6.6 (45.6)	5.2 (45.0)
Completeness (%)	99.9 (99.8)	94.5 (89.0)
Redundancy	3.5 (2.9)	4.8 (4.5)
<i>I</i> / <i>σ</i> (<i>I</i>)	25.0 (2.9)	29.9 (1.9)
Refinement		
Reflections used in refinement	47,869	36,594
σ Cutoff used in refinement	None	None
<i>R</i> / <i>R</i> _{free} ^c (%)	22.2/27.2	23.9/29.7
No. of refined atoms		
Protein	8,778	8,773
Waters	115	14
Folate		66
Ca ²⁺ cations	2	
Root mean square deviations		
Bond lengths (Å)	0.006	0.007
Bond angles (°)	1.2	1.3
Average B factor (Å ²)		
Protein	50.0	60.1
Folate		93.2

^a Values in parentheses are for the highest-resolution shell.

^b $R_{\text{sym}} = \sum |I_i - \langle I_i \rangle| / \sum I_i$, where I_i is the intensity of the i th observation and $\langle I_i \rangle$ is the mean intensity of the reflection.

^c $R = \sum \|F_o| - |F_c|\| / \sum |F_o|$, where F_o and F_c are the observed and calculated structure factors amplitudes. R_{free} is calculated using 4.7 and 4.3% of reflections omitted from the refinement for the GNMT apoprotein and GNMT-folate complex respectively.

liquor solution with the addition of 20% ethylene glycol as a cryoprotectant and frozen in liquid nitrogen. Diffraction data were collected at 100 K at Southeast Regional Collaborative Access Team (SER-CAT) beamline 22-BM, Advanced Photon Source, Argonne National Laboratory, using a MAR 225 CCD detector. The images were processed and scaled using HKL2000 (24). Data collection and data processing statistics are summarized in Table 1.

Structure Solution and Refinement—The structure of the apoGNMT was solved by the molecular replacement procedure as implemented in the CNS package (25). A dimer of the rat GNMT (Protein Data Bank (PDB) accession code 1BHJ) was used as the search model. Two dimers, which form a tetramer, were located in the asymmetric unit. The tetramer in the GNMT-folate structure was positioned using the rigid body refinement of the apoGNMT tetramer. The positioned tetrameric models of both the apo- and folate-bound structures were then refined using the maximum likelihood refinement in CNS (25). Two-fold non-crystallographic symmetry restraints and bulk solvent corrections were applied. The program O (26) was used to build the models throughout the refinement. Refinement statistics for both structures are listed in Table 1. Details of refinement of each of the structures follow.

GNMT Apoprotein—The final model consists of residues 2–196, 200–223, and 235–292 of subunit A, residues 1–227 and 235–292 of subunit B, residues 2–223 and 235–292 of subunit C, residues 1–227 and 233–292 of subunit D, two Ca²⁺ ions, and 115 water molecules. Residues C246 (subunit B) and R53 (subunit D) were modeled in two alternate conformations.

The molecules display good stereochemistry with 87.9% of non-glycine residues in the most favored regions of a Ramachandran plot and none in disallowed regions.

GNMT-Folate Complex—The difference Fourier map revealed the presence of two folate molecules in the tetramer of GNMT. They were modeled according to the shape of electron density. Their occupancy factor was set to 1. The final model consists of residues 2–196, 200–223, and 235–292 of subunit A, residues 1–227 and 235–292 of subunit B, residues 1–223 and 235–292 of subunit C, residues 1–227 and 233–292 of subunit D, two folates, and 14 water molecules. Similar to the apoprotein, 85.0% of non-glycine residues are in the most favored regions of a Ramachandran plot and none are in disallowed regions.

Other Methods—Protein concentration was routinely determined by the BCA method (BCA protein assay kit, Pierce) according to the manufacturer's protocol, with bovine serum albumin as a standard. In binding experiments, concentration was determined spectrophotometrically by using an absorbance value of 1.46 for a 0.1% solution at 278 nm in binding conditions. The latter was experimentally determined based on the value of 1.50 predicted from the amino acid composition for solution in 6 M guanidine hydrochloride. The BCA method gives a concentration 7.7% higher compared with the spectrophotometrically determined value; therefore, the coefficient of 0.929 was used to obtain the correct concentration.

Protein purity was determined by standard SDS electrophoresis with scanning of the Coomassie-stained gel on Bio-Rad Gel/Chemi Doc system and Quantity One software. Microbiological assay for folate was done by the *Lactobacillus casei* microbiological assay according to a published procedure (27). Absorbance spectra were recorded on a double beam Shimadzu UV-2401 spectrophotometer.

RESULTS

Folate Binding to GNMT—The binding data are presented in Fig. 2 as the dependence of the molar ratio of folate bound to GNMT (tetramer) on the concentration of free folate [F_{free}]. Fitting the data by the equation described under "Folate Binding" gave the value of the ratio of $[F_{\text{bound}}]/[\text{GNMT}_{\text{tet}}] = 2$ (1.944). That means that one molecule of GNMT tetramer binds two molecules of folate. The value of the association constant K_A was calculated to be $3.42 \times 10^5 \times \text{M}^{-1}$ (or 2.9 μM for K_D). The latter means that crystallization experiments should be performed at a millimolar concentration of folate to follow a general suggestion to use a ligand concentration of 1000-fold higher than K_D .

Crystallization—The major requirements for crystallization conditions were to maintain a pH of >7 for effective folate binding to GNMT in the ionization state similar to physiologic conditions and the presence of reducing agent to prevent oxidative degradation of 5-CH₃-H₄PteGlu. Several crystallization conditions were found to be favorable for GNMT-folate complex crystal growth. The best crystals were obtained in the presence of calcium-acetate in 20% polyethylene glycol 3350 (Fig. 3A) and a folate concentration of 1–3 mM with 5 mM TCEP. In those conditions, crystals of GNMT-folate complex appeared

GNMT-Folate Structure

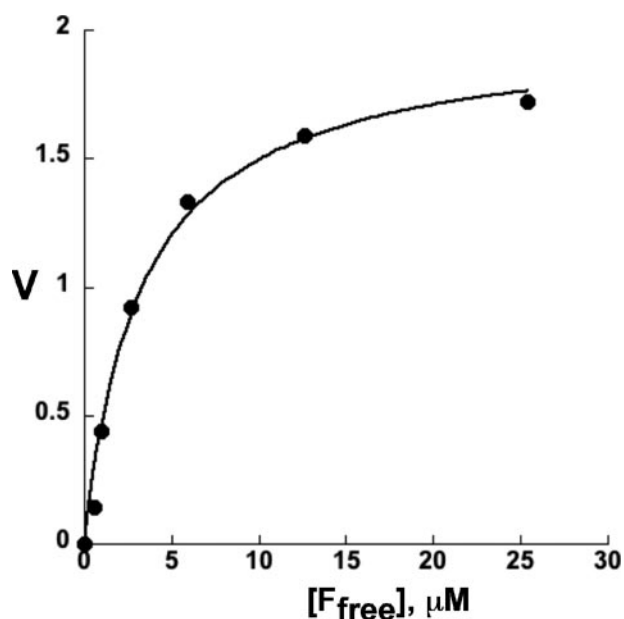


FIGURE 2. **Binding of 5-CH₃-H₄PteGlu by rat GNMT.** Rat recombinant GNMT incubated with folate of different concentrations in 20 mM Tris-HCl, 25 mM NaCl, 5 mM TCEP, pH 7.5, 1 h on ice. Part of the solution was separated from protein by filtration, and the concentration of free folate was measured by absorbance at 290 nm. The molar ratio of bound folate/GNMT tetramer (V) calculated and plotted against free folate concentration. Fitted value for n is 1.944 and for K_A is $3.42 \times 10^5 \text{ M}^{-1}$.

in hours. The shape of the crystals for the complex was as shown in Fig. 3A.

One of the critical points of this work was obtaining crystals of GNMT apoprotein grown under the same conditions as for the GNMT-folate complex. Such crystals give the best comparison of crystal structures of the folate-free protein and the GNMT-folate complex, avoiding any question of potential effects of different components of the precipitants and buffers. The latter was of special importance, because GNMT is known for its ability to trap some components of the crystallization media (14). In most cases, the apoprotein crystals were grown in the form of tiny needles not suitable for data collection (Fig. 3B). However, in two drops in calcium-acetate, two plate-shaped crystals of GNMT apoprotein grew to a relatively large size.

The presence of folate in the GNMT-folate complex crystals was confirmed by microbiological assay (27). Additional evidence for the presence of folate in the GNMT-folate crystals was an observation that crystals, after five months of storage in mother liquor, became yellow- and red-colored, and the intensity of the color increased over time, yet the mother liquor remained clear (Fig. 3C). None of the crystals of GNMT without folate became colored, even after storage for a year in the mother liquor. The red color could be explained by a shift of the absorbance spectra to $>400 \text{ nm}$ due to folate oxidation to a still unidentified "red product" (28, 29). None of the GNMT-folate complex crystals were used for data collection later than one week after crystal growth initiation.

Overall Structures—The asymmetric unit in the folate-free as well as the GNMT-folate complex is represented by a tetramer in a so-called closed conformation. Important features of that structure are the positions of the N-terminal



FIGURE 3. **Crystals of rat GNMT.** A, GNMT-folate complex. B, apoprotein. C, GNMT-folate crystals after six months of storage in crystallization solution.

fragments of the subunits, which were found interacting with residues of the entrance into the active center of the adjacent subunits (16, 17).

The overall conformation did not change upon folate binding. Folate-free and folate-bound structures are very similar, with root mean square deviations of 0.738 \AA over the 1129 equivalent CA atoms. In addition, flexible parts of the protein molecules (parts of protein model for which no electron density has been observed) are almost identical and similar to those found in the structures of human and mouse GNMTs (14).

Despite a very similar overall structure, there are some differences. An important one is a difference in the conformations of Tyr⁵ residues, especially Tyr⁵ (A) and Tyr⁵ (D). In the GNMT-folate complex, those tyrosine residues play an important role in folate binding.

Localizing the Folate Binding Sites—The principal goal of this work was to localize the folate binding sites in the rat GNMT. Difference Fourier electron density map contoured at 4σ for the GNMT-folate complex revealed the presence of two areas of additional electron density located in the intersubunit area (Fig. 4A). The shape of the density was consistent with a folate molecule. On the contrary, no additional electron density has been observed in the same area for the apoprotein (Fig. 4B). Because the binding experiment showed that the GNMT tetramer binds two folate molecules, it was concluded that the additional electron density originated from folate.

Folate Conformation—Folates and their derivatives exist in complexes with proteins in different conformations with different relative orientation of the pteridine ring, *p*-aminobenzoyl (PABA) group, and glutamate residue(s), which depend on the specific folate-protein interactions (30, 31). Two general conformations of folates were found. The most abundant one is the bent conformation, as found in dihydrofolate reductase and other enzymes (32). In crystal structures of enzymes with 5-CH₃-H₄PteGlu and with 5-CH₃-H₄PteGlu₅, some contain folate in the bent conformation, whereas others contain folate in the extended form (32–35). The best assignment of the folate in the electron density in the GNMT-folate complex was achieved when the folate was built in almost extended conformation as shown in Fig. 5.

Folate-Protein Interactions—The folate conformation is supported by specific folate-GNMT interactions. The interaction of folate with the GNMT protein moiety followed the general rule for the folate-protein interaction; the pteridine and *p*-aminobenzoyl rings were buried into the more hydrophobic inte-

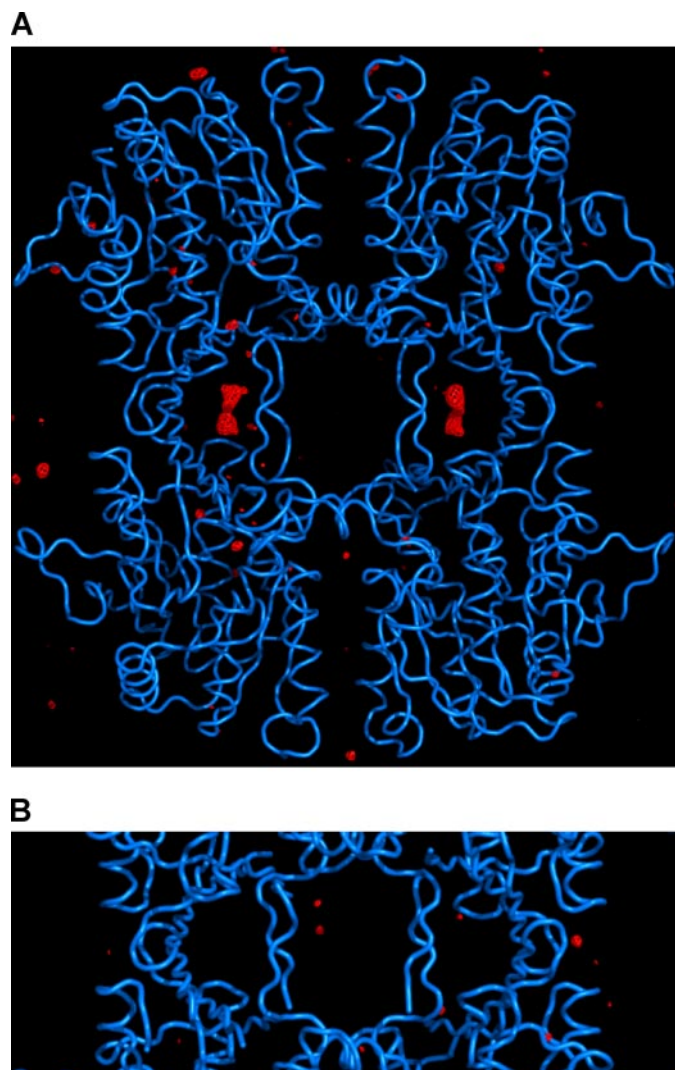


FIGURE 4. Difference Fourier electron density maps contoured at 4σ calculated for the GNMT-folate (A) and GNMT apoprotein (B) structures. Two areas of additional extended electron density in the map of the GNMT-folate complex are clearly visible. No additional electron density was found on the GNMT apoprotein map. In B, only the central part of the map and model is shown.

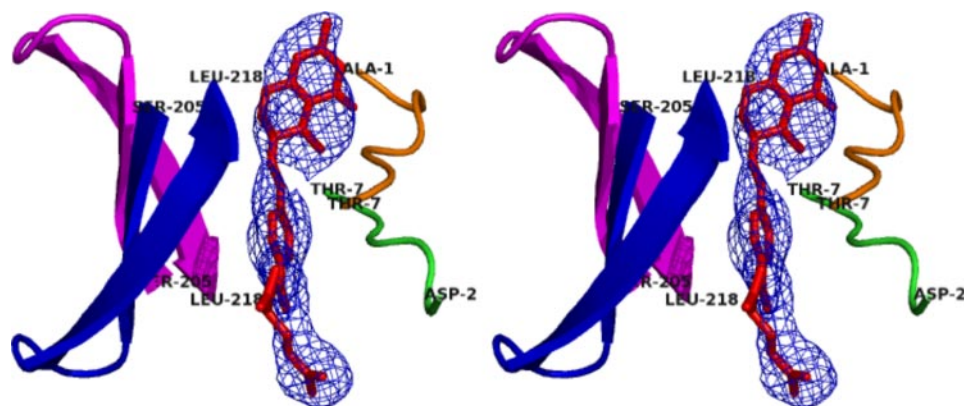


FIGURE 5. Stereo view of folate-protein secondary structure interactions and position of folate in electron density map. The relative positions of the folates and elements of the secondary structure of the protein in the folate binding site 1 are shown. The fragments from subunits A, B, C, and D are colored as in Fig. 1. Electron density $F_o - F_c$ simulated annealed, omitting the 2.55 Å resolution map for the omitted folate molecule calculated at 4 Å, is shown.

rior of the protein with the glutamate tail exposed to the surface of the protein globule. The characteristic feature of folate-GNMT binding is that the folate binding sites are located in very specific parts of the quaternary structure of GNMT in the intersubunit areas.

As shown in Fig. 5, binding site 1 is located between subunits B and D in the cavity formed by two interacting parts of all four subunits, two β -sheets formed by residues Ser²⁰⁵-Thr²¹⁸ (B) and Ser²⁰⁵-Thr²¹⁸ (D) on the one side and two N-terminal fragments including residues Asp²-Thr⁷ (A) and Val¹-Thr⁷ (C) on the other side. Binding site 2 is related by 2-fold non-crystallographic symmetry to site 1 and is located between subunits A and C. This site is formed by similar elements of the polypeptide chains as for binding site 1, two β -sheets formed by residues of Ser²⁰⁵-Thr²¹⁸ (A) and Ser²⁰⁵-Thr²¹⁸ (C) and two N-terminal fragments Val¹-Thr⁷ (B) and Val¹-Thr⁷ (D).

The specific interactions are shown in Fig. 6 and in Table 2 for binding site 1, having in mind that similar interactions exist in the site 2. Folate molecules are stabilized inside of a tetramer by mainly hydrophobic interactions with only one hydrogen bond observed. Such a feature explains the relatively high B-factors of folates, which are 1.5 times higher than the average B-factors of protein molecules (Table 1). Within a distance of 4.0 Å from the folate there are residues Ser³ (C), Tyr⁵ (A, C), Thr⁷ (C), Leu²⁰⁷ (B, D), His²¹⁴ (D), Met²¹⁵ (B, D), and Arg²³⁹ (B). The hydrophobic pocket of binding site 1 is formed primarily by Tyr⁵, Leu²⁰⁷, His²¹⁴, and Met²¹⁵ residues (Table 2).

The pteridine ring interacts with the protein mainly by hydrophobic contacts. There are numerous such contacts (a total of 15 as determined by the Ligand Explorer program (36)) that involve Tyr⁵ (C) with close contact to C7 of the pteridine, the methyl groups of Leu²⁰⁷ (B), which are at a distance of 2.9 Å from C7 pteridine and others as shown in Table 2. The 5-methyl group of folate is directed into a hydrophobic cavity of GNMT with the closest distance to the methyl group of Thr⁷ (A) (3.4 Å) and the methylene group of Tyr⁵ (C) (3.5 Å).

The PABA moiety of folate is placed in the most hydrophobic part of the binding site (with 19 hydrophobic contacts) as shown in Fig. 6 and Table 2. Tyr⁵ (A) and Leu²⁰⁷ (D) give the main yield in hydrophobic interactions with PABA (17 contacts). There is also a possibility for polar interaction, because the NH₂ group of Arg²³⁹ (B) is a distance of 3.6 Å from the C=O group of PABA.

The glutamate part of the folate participates in the most specific interactions with protein. The only hydrogen bond between folate and protein is established between the γ -carboxyl group of glutamate and the hydroxyl group of Tyr⁵ (A) with a distance of 3.2 Å (Fig. 6) (3.0 Å in site 2). The α -carboxyl group is involved in interaction with the sul-

GNMT-Folate Structure

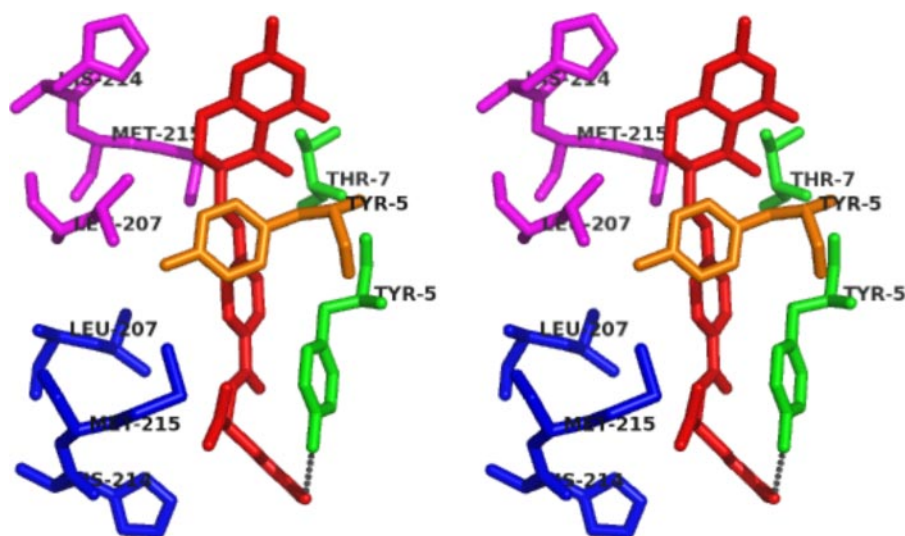


FIGURE 6. Stereo view of folate interactions with amino acid residues in the binding site 1. The residues, within 4 Å distance from folate with a major yield into folate-protein interactions are shown. The residues are colored as in Fig. 1. The dotted line indicates the hydrogen bond. The distances between specific groups and atoms of folate and protein are presented in Table 2.

TABLE 2

5-CH₃-H₄-PteGlu – GNMT interactions

Total hydrophobic contacts of folate-protein is 45, hydrogen bonds –1. Only selected contacts are presented.

5-CH ₃ -H ₄ -PteGlu	GNMT atom/ group-residues (subunit)	Distance
		Å
Pteridine		
C4	CB-Ser ³ (C)	3.68
C6	CE-Met ²¹⁵ (B)	3.69
C7	CD2-Leu ²⁰⁷ (B)	2.91
C7	CD1-Tyr ⁵ (C)	3.26
5-CH ₃	CB-Tyr ⁵ (C)	3.53
5-CH ₃	CG2-Thr ⁷ (A)	3.41
PABA		
C12	CB, CG-Tyr ⁵ (A)	3.44, 3.46
C13	CB, CG-Tyr ⁵ (A)	3.38, 3.88
C17	CD2-Leu ²⁰⁷ (D)	3.88
CO	NH ₂ -Arg ²³⁹ (B)	3.59
Glutamate		
α-COO	S-Met ²¹⁵ (D)	3.10, 3.25
α-COO	ND1-His ²¹⁴ (D)	3.41
γ-COO	HO-Tyr ⁵ (A), H-bond	3.19 (3.0 in site 2)
CA	CZ-Tyr ⁵ (A)	3.68
CB	CZ-Tyr ⁵ (A)	3.11

fur atom of Met²¹⁵ (D) with a distance between oxygens and sulfur atoms of 3.10 and 3.25 Å. Interestingly, there are also 13 hydrophobic contacts of glutamate with Tyr⁵, Leu²⁰⁷, and His²¹⁴.

DISCUSSION

Glycine *N*-methyltransferase is a major liver regulatory enzyme that plays a key role in maintaining one of the most important cell parameters, the AdoMet/AdoHcy ratio, often referred to as the methylation index. In cases when GNMT was inactivated by missense mutations in humans (5, 6) or completely knocked out by gene targeting in mice (7), the concentrations of critically important metabolites, methionine, and AdoMet in human plasma and in mice liver were extremely high. The latter leads to damage of the liver and liver disease.

GNMT is also a major liver cytosolic folate-binding protein. Its high abundance in the liver (4) results in the major portion (if

not all) of 5-methyltetrahydrofolate tightly bound to GNMT (8). It should be noted that GNMT is abundant in other tissues, *e.g.* in the pancreas, prostate, and kidney. Binding of and inhibition by folate is a key part of the mechanism of control of the AdoMet/AdoHcy ratio during the lifetime of the organism. The crystal structure of the GNMT-folate complex we are reporting here gives insight into the mechanism of that regulation.

How is GNMT inhibited by folate? The crystal structure of GNMT complexed with 5-methyltetrahydrofolate revealed that bound folate does not directly interfere with binding of AdoMet by competing for the active center. AdoMet is bound to the active site on each subunit deep into the monomer globule as shown earlier (Fig. 1) (15–17). The AdoMet binding mechanism deduced from the crystal structure of rat GNMT with AdoMet indicated that the N-terminal domain of each subunit had moved out of the position where it was blocking the entrance to the active site of the adjacent subunit. The N-terminal fragments then became exposed to solvent (17).

As a result of those rearrangements of the N-terminal fragments of GNMT, the cavities for folate binding are not formed and folate cannot bind to GNMT when the active sites are occupied with AdoMet. The data presented here show explicitly that, when folate is already bound to GNMT, the N-terminal fragments are bound to folate and their move from the protein globule into the solvent to gain access for AdoMet requires much higher concentrations of AdoMet compared with apoprotein.

Inhibition experiments (37) support this mechanism. It was found that 5-methyltetrahydrofolate pentaglutamate inhibited rat GNMT efficiently if it was incubated with protein prior to the addition of AdoMet and other components of the reaction mixture. Obviously, this situation was a result of the difference in the binding constants for AdoMet and folate and the energy required for protein conformational changes that accompany the exposure of the N-terminal parts of the monomers from the globule into the solvent. It should be noted that these earlier experiments indicated that there was only a single molecule of folate bound per tetramer. They were carried out using fluorescence determination of the free and total bound folate, and the calculation employed Scatchard analysis, a much less rigorous procedure. In addition, the form of folate used in these earlier studies was the pentaglutamate. It is possible, but unlikely, that the different result was because of the length of the polyglutamate chain.

Localization of the folate binding sites in the rat GNMT is important in understanding the mechanism of inhibition of this enzyme by folate, which is responsible for regulating the methylation status of the cell. The data presented here are likely valid

for GNMT from other sources. All residues participating in folate binding in the rat GNMT are invariant in the protein sequences of GNMTs from rat, human, rabbit, pig, and mouse (14, 38).

Acknowledgments—We thank the Vanderbilt University Center for Structural Biology for access to the Biomolecular Crystallography Facilities. Data were collected at Southeast Regional Collaborative Access Team 22-BM beamline at the Advanced Photon Source, Argonne National Laboratory. Use of the Advanced Photon Source was supported by the United States Department of Energy, Office of Science, Office of Basic Energy Sciences, under Contract No. W-31-109-Eng-38. We also thank Merck EPROVA (Switzerland) for free samples of folate.

REFERENCES

- Cantoni, G. L., Richards, H. H., and Chiang, P. K. (1978) in *Transmethylation* (Usdin, E., Borchardt, R.T., and Creveling, C.R., eds) pp. 155–164, Elsevier, New York
- Clarke, S., and Banfield, K. (2001) in *Homocysteine in Health and Disease* (Carmel, R., and Jacobsen, D.W., eds) pp. 63–78, Cambridge University Press, Cambridge, UK
- Blumenstein, J., and Williams, G. R. (1960) *Biochem. Biophys. Res. Comm.* **3**, 259–263
- Heady, J. E., and Kerr, S. J. (1973) *J. Biol. Chem.* **248**, 69–72
- Mudd, S. H., Cerone, R., Schiaffino, M. C., Fantasia, A. R., Manniti, G., Caruso, U., Lorini, R., Watkins, D., Matiaszuk, N., Rosenblatt, D. S., Schwahn, B., Rozen, R., LeGros, L., Kotb, M., Capdevila, A., Luka, Z., Finkelstein, J. D., Tangerman, A., Stabler, S. P., Allen, R. H., and Wagner, C. (2001) *J. Inher. Metab. Dis.* **24**, 448–464
- Luka, Z., Cerone, R., Phillips, J. A., III, Mudd, S. H., and Wagner, C. (2002) *Hum. Genet.* **110**, 68–74
- Luka, Z., Capdevila, A., Mato, J. M., and Wagner, C. (2006) *Transgenic Res.* **15**, 393–397
- Zamierowski, M. M., and Wagner, C. (1977) *J. Biol. Chem.* **252**, 933–938
- Suzuki, N., and Wagner, C. (1980) *Arch. Biochem. Biophys.* **199**, 236–248
- Cook, R. J., and Wagner, C. (1984) *Proc. Natl. Acad. Sci. U. S. A.* **81**, 3631–3634
- Wagner, C., Briggs, W. T., and Cook, R. J. (1985) *Biochem. Biophys. Res. Commun.* **127**, 746–752
- Balaghi, M., Horne, D. W., Woodward, S. C., and Wagner, C. (1993) *Am. J. Clin. Nutr.* **58**, 198–203
- Pattanayek, R., Newcomer, M. E., and Wagner, C. (1998) *Protein Sci.* **7**, 1326–1331
- Pakhomova, S., Luka, Z., Grohmann, S., Wagner, C., and Newcomer, M. E. (2004) *Proteins Struct. Funct. Bioinform.* **57**, 331–337
- Fu, Z., Hu, Y., Konishi, K., Takata, Y., Ogawa, H., Gomi, T., Fujioka, M., and Takusagawa, F. (1996) *Biochemistry* **35**, 11985–11993
- Huang, Y., Komoto, J., Konishi, K., Takata, Y., Ogawa, H., Gomi, T., Fujioka, M., and Takusagawa, F. (2000) *J. Mol. Biol.* **298**, 149–162
- Takata, Y., Huang, Y., Komoto, J., Yamada, T., Konishi, K., Ogawa, H., Gomi, T., Fujioka, M., and Takusagawa, F. (2003) *Biochemistry* **42**, 8394–8402
- Chen, S.-Y., Lin, J.-R. V., Darbha, R., Lin, P., Liu, T.-Y., and Chen, Y.-M. A. (2004) *Cancer Res.* **64**, 3617–3623
- Luka, Z., and Wagner, C. (2003) *Protein Expression Purif.* **20**, 280–286
- Blakley, R. L. (1969) *The Biochemistry of Folic Acid and Related Pteridines*, Wiley & Sons, Inc., New York
- Gupta, V. S., and Huenekens, F. M. (1967) *Arch. Biochem. Biophys.* **120**, 712–718
- Klotz, I. M. (1946) *Arch. Biochem.* **9**, 109–117
- Brautigam, C. A., Smith, B. S., Ma, Z., Palnitkar, M., Tomchick, D. R., Machius, M., and Deisenhofer, J. (2004) *Proc. Natl. Acad. Sci. U. S. A.* **101**, 12142–12147
- Otwinowski, Z., and Minor, W. (1997) *Methods Enzymol.* **276**, 307–326
- Adams, P. D., Pannu, N. S., Read, R. J., and Brunger, A. T. (1997) *Proc. Natl. Acad. Sci. U. S. A.* **94**, 5018–5023
- Jones, T. A., Zou, J. Y., Cowan, S. W., and Kjeldgaard, M. (1991) *Acta Crystallogr. Sect. A* **47**, 110–119
- Horne, D. W., and Patterson, D. (1988) *Clin. Chem.* **34**, 2357–2359
- Thomas, A. H., Suarez, G., Cabrerizo, F. M., and Capparelli, A. L. (2001) *Helv. Chim. Acta* **84**, 3849–3860
- Thomas, A. H., Suarez, G., Cabrerizo, F. M., Einschlag, F. S. G., Martino, R., Baiocchi, C., Pramauro, E., and Capparelli, A. L. (2002) *Helv. Chim. Acta* **85**, 2300–2315
- Poe, M., and Benkovic, S. J. (1980) *Biochemistry* **19**, 4576–4582
- Cody, V., Luft, J. R., Pangborn, W., Gangjee, A., and Queener, S. F. (2004) *Acta Crystallogr. Sect. D Biol. Crystallogr.* **60**, 646–655
- Matthews, D. A., Alden, R. A., Bolin, J. T., Freer, S. T., Hamlin, R., Xuong, N., Kraut, J., Poe, M., Williams, M., and Hoogsteen, K. (1977) *Science* **197**, 452–455
- Hyatt, D. C., Maley, F., and Montfort, W. R. (1997) *Biochemistry* **36**, 4585–4594
- Pejchal, R., Sargeant, R., and Ludwig, M. L. (2005) *Biochemistry* **44**, 11447–11457
- Evans, J. C., Huddler, D. P., Hilgers, M. T., Romanchuk, G., Matthews, R. G., and Ludwig, M. L. (2004) *Proc. Natl. Acad. Sci. U. S. A.* **101**, 3729–3736
- Moreland, J. L., Gramada, A., Buzko, O. V., Zhang, Q., and Bourne, P. E. (2005) *BMC Bioinformatics* **6**, 21
- Yeo, E.-J., Briggs, W. T., and Wagner, C. (1999) *J. Biol. Chem.* **274**, 37559–37564
- Ogawa, H., Gomi, T., and Fujioka, M. (1993) *Comp. Biochem. Physiol. B.* **106**, 601–611